Intestinal myofibroblast-specific Tpl2-Cox-2-PGE_2 pathway links innate sensing to epithelial homeostasis

Manolis Roulis[a,1], Christoforos Nikolaou[a], Elena Kotsaki[a], Eleanna Kaffe[a], Niki Karagianni[b], Vasiliki Koliaraki[a], Klelia Salpea[a], Jiannis Ragoussis[a,c], Vassilis Aidinis[a], Eva Martini[d], Christoph Becker[d], Harvey R. Herschman[e], Stefania Vetrano[f], Silvio Danese[f], and George Kollias[a,1]

[a]Institute of Immunology, Biomedical Sciences Research Center "Alexander Fleming", Vari 16672, Greece; [b]Biomedcode Hellas SA, Vari 16672, Greece; [c]McGill University and Genome Quebec Innovation Center, Montreal, QC, Canada H3A 0G1; [d]Department of Medicine 1, Friedrich-Alexander-University, 91052 Erlangen, Germany; [e]David Geffen School of Medicine, University of California, Los Angeles, CA, 90095-1570; and [f]Inflammatory Bowel Disease Center, Humanitas Clinical and Research Center, 20089 Rozzano, Italy

Edited by Philippe J. Sansonetti, Institut Pasteur, Paris, France, and approved September 19, 2014 (received for review August 22, 2014)

Tumor progression locus-2 (Tpl2) kinase is a major inflammatory mediator in immune cell types recently found to be genetically associated with inflammatory bowel diseases (IBDs). Here we show that Tpl2 may exert a dominant homeostatic rather than inflammatory function in the intestine mediated specifically by subepithelial intestinal myofibroblasts (IMFs). Mice with complete or IMF-specific Tpl2 ablation are highly susceptible to epithelial injury-induced colitis showing impaired compensatory proliferation in crypts and extensive ulcerations without significant changes in inflammatory responses. Following epithelial injury, IMFs sense innate or inflammatory signals and activate, via Tpl2, the cyclooxygenase-2 (Cox-2)-prostaglandin E_2 (PGE_2) pathway, which we show here to be essential for the epithelial homeostatic response. Exogenous PGE_2 administration rescues mice with complete or IMF-specific Tpl2 ablation from defects in crypt function and susceptibility to colitis. We also show that Tpl2 expression is decreased in IMFs isolated from the inflamed ileum of IBD patients indicating that Tpl2 function in IMFs may be highly relevant to human disease. The IMF-mediated mechanism we propose also involves the IBD-associated genes *IL1R1*, *MAPK1*, and the PGE_2 receptor-encoding *PTGER4*. Our results establish a previously unidentified myofibroblast-specific innate pathway that regulates intestinal homeostasis and may underlie IBD susceptibility in humans.

Crohn's disease | ulcerative colitis | mesenchymal cells | MAP kinases | cyclooxygenase-2

Inflammatory bowel diseases (IBDs), encompassing Crohn's disease and ulcerative colitis, are chronic inflammatory disorders of the gastrointestinal tract that develop from a complex and largely unknown etiology (1). Recent genome-wide association studies (GWAS) for IBD showed significant association with SNP rs1042058 in mitogen-activated protein kinase kinase kinase 8 (*MAP3K8*) gene (2) which encodes tumor progression locus-2 (Tpl2) kinase (*SI Appendix*, Fig. S1 *A* and *B*). Molecularly, Tpl2 is known to bind to NF-κB1-p105 in a stabilized but inactive form (3) and, when activated, is released to phosphorylate the major immediate targets MEK1/2 activating mainly the ERK pathway and downstream inflammatory mediators (3). The *NFKB1* gene is also genetically associated with IBD in GWAS (2), highlighting the relevance of this pathway to human disease. $Tpl2^{-/-}$ mice show defective TNF expression in response to LPS (4), high susceptibility to *Listeria* due to defective IL-1β expression (5), and impaired Th1 responses (6). Tpl2 also mediates pathogenesis in the TNF-driven and T-cell–mediated $Tnf^{\Delta ARE}$ mouse model of Crohn's-like IBD, indicating a potential pathogenic relevance of this pathway in specific contexts (7). Due to these proinflammatory functions, established mainly in cells of hematopoietic origin, Tpl2 is considered to be an appealing pharmacological target for the treatment of IBD and other inflammatory diseases (3, 8).

The genetic association of *MAP3K8* with IBD, however, may indicate unknown homeostatic functions of Tpl2 in the intestine. GWAS results provide insights into the complexity underlying *MAP3K8* association because along with *NFKB1*, an additional 25 genes functionally related to Tpl2 are genetically associated with IBD (2). These functional interactions can be clustered in a wide spectrum of cell types and potential mechanisms (*SI Appendix*, Fig. S2 *A* and *B* and Table S1). Indeed, Tpl2 functions in many different cell types downstream of receptors such as CD40 (9), CD3/CD28 (10), TNFRI (11), IL-1R (11), NOD2 (5), or TLR4 (4). Notably, these pathways may have opposing roles in intestinal homeostasis and IBD; for example, contrasting homeostatic and epithelial cell death-promoting roles have been suggested for TLR4 and TNFRI, respectively (12, 13). A cell-specific approach is therefore required for detailed mechanistic understanding of the role of Tpl2 in IBD and effective therapeutic design.

Here, studying the role of Tpl2 in intestinal homeostasis and IBD pathogenesis in a cell-specific manner, we identify a myofibroblast-specific Tpl2-Cox-2-PGE_2 pathway which plays a

Significance

Tumor progression locus-2 (Tpl2) is a proinflammatory gene genetically associated with inflammatory bowel diseases. This study provides a mechanistic interpretation for this association showing a dominant Tpl2-mediated homeostatic mechanism protecting mice from epithelial injury-induced colitis. This function of Tpl2 is mediated specifically by subepithelial intestinal myofibroblasts, a cell type supporting crypt stem cells. Tpl2 in myofibroblasts is essential for the compensatory proliferative response of the epithelium by promoting arachidonic acid metabolism and cyclooxygenase-2 (Cox-2)/prostaglandin E_2 activation. Notably, in Crohn's Disease patients, Tpl2 is downregulated in myofibroblasts isolated from the inflamed ileum. These results challenge current concepts on a solely proinflammatory function of Tpl2 and highlight the dominant role of subepithelial myofibroblasts in sensing inflammation and tissue damage and promoting intestinal homeostasis through Tpl2-Cox-2-prostaglandin E_2.

Author contributions: M.R. and G.K. designed research; J.R. implemented RNA-seq; E. Kaffe and V.A. implemented eicosanoid analysis; M.R., N.K., V.K., E.M., and C.B. performed research; G.K. supervised research; H.R.H. contributed Cox-2 conditional knockout mice; M.R. analyzed data; C.N. analyzed RNA-seq data; E. Kotsaki made the Tpl2 targeting vector; K.S. prepared RNA-seq libraries; S.V. and S.D. isolated intestinal myofibroblasts from a cohort of patients; and M.R. and G.K. wrote the paper.

The authors declare no conflict of interest.

This article is a PNAS Direct Submission.

[1]To whom correspondence may be addressed. Email: kollias@fleming.gr or roulis@fleming.gr.

This article contains supporting information online at www.pnas.org/lookup/suppl/doi:10.1073/pnas.1415762111/-/DCSupplemental.

homeostatic role in the gut by promoting the compensatory proliferative response of the epithelium upon injury. This mechanism highlights the dominant role of IMFs in regulating epithelial homeostasis and also provides a possible explanation for the *MAP3K8* association with IBD (see Fig. 8).

Results

Tpl2 Plays a Homeostatic Role in the Gut Following Epithelial Injury. To study the cell-specific functions of Tpl2 we generated Tpl2 conditional (floxed, $Tpl2^{FL/FL}$) and complete knockout mice (defloxed, $Tpl2^{D/D}$) as described in *Materials and Methods* and *SI Appendix*, Fig. S3. To investigate the role of Tpl2 in intestinal homeostasis and IBD pathogenesis we used the DSS-induced colitis model which is based on epithelial barrier disruption involving mainly innate immune responses (14) and activation of epithelial repair mechanisms. We observed that $Tpl2^{D/D}$ mice are highly susceptible to DSS-induced colitis exhibiting significantly increased weight loss, disease activity index, and lethality and reduced colon length compared with normal littermate controls (Fig. 1 *A–D*). $Tpl2^{D/D}$ mice also display exacerbated histopathological features of colitis with increased loss of Goblet cells, extensive loss of crypts, and focal ulceration at an early time point (Fig. 1 *E–G*), progressing later to severe and widely spread ulceration (Fig. 1 *E* and *F*). $Tpl2^{D/D}$ mice show throughout the DSS-induced colitis protocol significantly increased tissue damage histological score as reflected in loss of crypts and ulceration (Fig. 1*H*) but similar inflammation scores compared with WT controls (Fig. 1*H*). These results show that Tpl2 plays an unexpected homeostatic role in the intestine following epithelial injury.

Tpl2 Is Dispensable for Inflammatory Infiltration but Critically Implicated in Mechanisms of Epithelial Homeostasis upon Epithelial Injury. FACS analysis in isolated colonic lamina propria and mesenteric lymph node populations showed similar infiltrations of macrophages and granulocytes in $Tpl2^{D/D}$ and WT mice early upon epithelial injury (Fig. 2 *A* and *B* and *SI Appendix*, Fig. S4*B*). In addition, no differences were observed in myeloperoxidase activity (Fig. 2*C*) or in the expression of several inflammatory cytokines and chemokines in the colons of these mice (*SI Appendix*, Fig. S4 *C* and *D*). Similar results in terms of inflammatory activation and myeloperoxidase activity were obtained at a later time point (*SI Appendix*, Fig. S5). Examination of immune and cytokine secretion pathways in which Tpl2 has been demonstrated to be involved in vivo (6, 15, 16) showed that Th1 and Th17 responses, IL-10 secretion from $CD4^+$ T cells, and IFN-γ secretion from $CD8^+$ T cells were similar in the lamina propria of $Tpl2^{D/D}$ and WT mice (*SI Appendix*, Fig. S4*A*). This observation is possibly related to the predominance of innate pathways in the DSS model (14). The above results suggest that in the context of DSS colitis, Tpl2 is dispensable for the development of inflammatory responses. On the other hand, the accelerated loss of crypts in DSS-treated $Tpl2^{D/D}$ mice suggests a possible involvement of Tpl2 in the mechanisms of epithelial homeostasis including epithelial proliferation, migration, differentiation, and cell death. TUNEL assays in the colon of DSS-treated $Tpl2^{D/D}$ and WT control mice showed a similar extent of spontaneous epithelial apoptosis (*SI Appendix*, Fig. S6 *A* and *B*). Because aberrant intestinal epithelial cell (IEC) death requires IEC sensitization to TNF (13, 17) and Tpl2 mediates TNFRI signaling (3), we also performed TUNEL assays in the intestine of TNF-injected $Tpl2^{D/D}$ and WT mice and excluded an implication of Tpl2 in TNF-induced

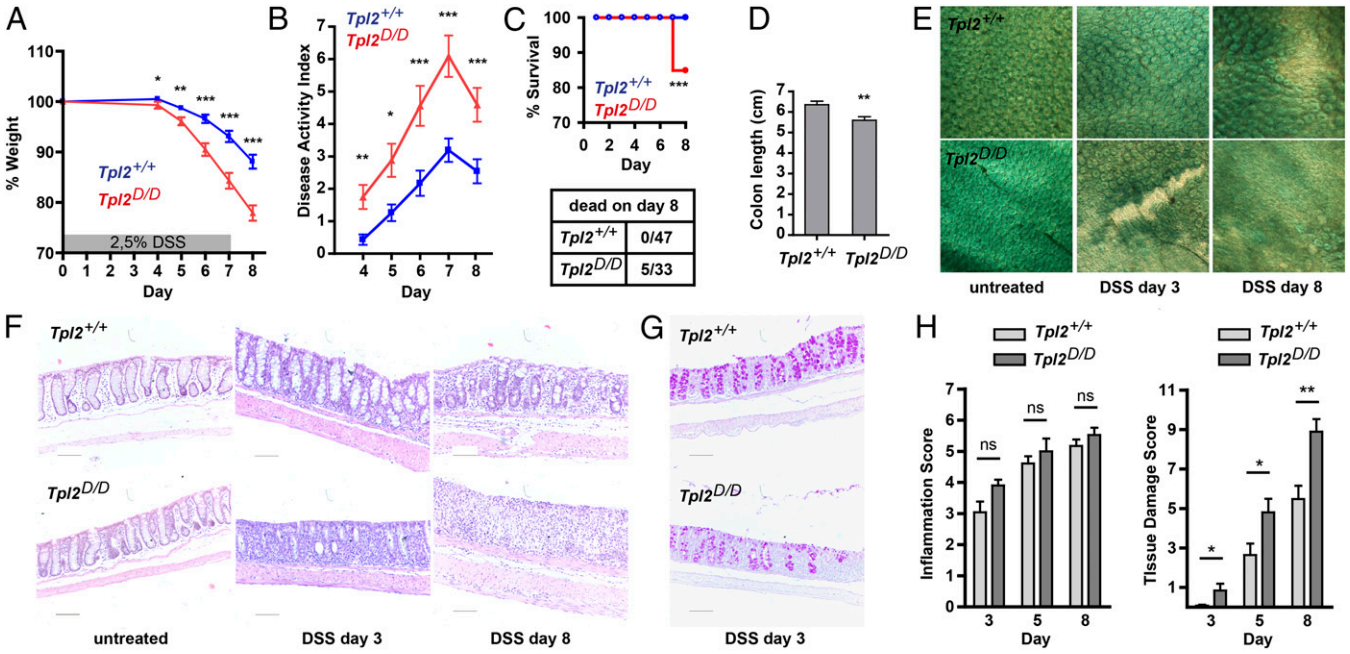

Fig. 1. Tpl2 deficient mice are highly susceptible to dextran sodium sulfate (DSS)-induced colitis. (*A–C*) $Tpl2^{D/D}$ ($n = 32$) and WT control mice ($n = 47$) were treated with 2.5% DSS in five independent experiments. $Tpl2^{D/D}$ mice showed (*A*) increased weight loss, (*B*) increased disease activity index, and (*C*) increased lethality ($P = 0.00258$; Gehan–Wilcoxon test) compared with WT controls. (*D*) $Tpl2^{D/D}$ mice ($n = 19$) showed reduced colon length on experimental day 8 compared with WT control mice ($n = 33$) in three independent experiments. (*E*) Methylene blue staining of colon whole mounts from DSS-treated $Tpl2^{D/D}$ and WT control mice on days 3 and 8. $Tpl2^{D/D}$ mice show early loss of crypts and focal ulceration on day 3, progressing later to widespread ulceration. (Magnification: 100×.) (*F*) $Tpl2^{D/D}$ mice show early loss of crypts on day 3 progressing later to complete loss of crypts and extensive ulceration on day 8. H&E-stained colon sections. (Scale bars: 100 μm.) (*G*) Early loss of Goblet cells in $Tpl2^{D/D}$ mice as shown by periodic acid-Schiff staining. (Scale bars: 100 μm.) (*H*) Histopathological analysis of DSS-treated $Tpl2^{D/D}$ and WT control mice early on day 3 ($n = 5$ and 6, respectively), on day 5 ($n = 7$ and 9), and late on day 8 ($n = 11$ and 18). All data shown represent mean ± SEM. Statistical significance was calculated with Student *t* test, Welch's *t* test, or Mann–Whitney test (*$P < 0.05$; **$P < 0.01$; ***$P < 0.001$; ns, nonsignificant).

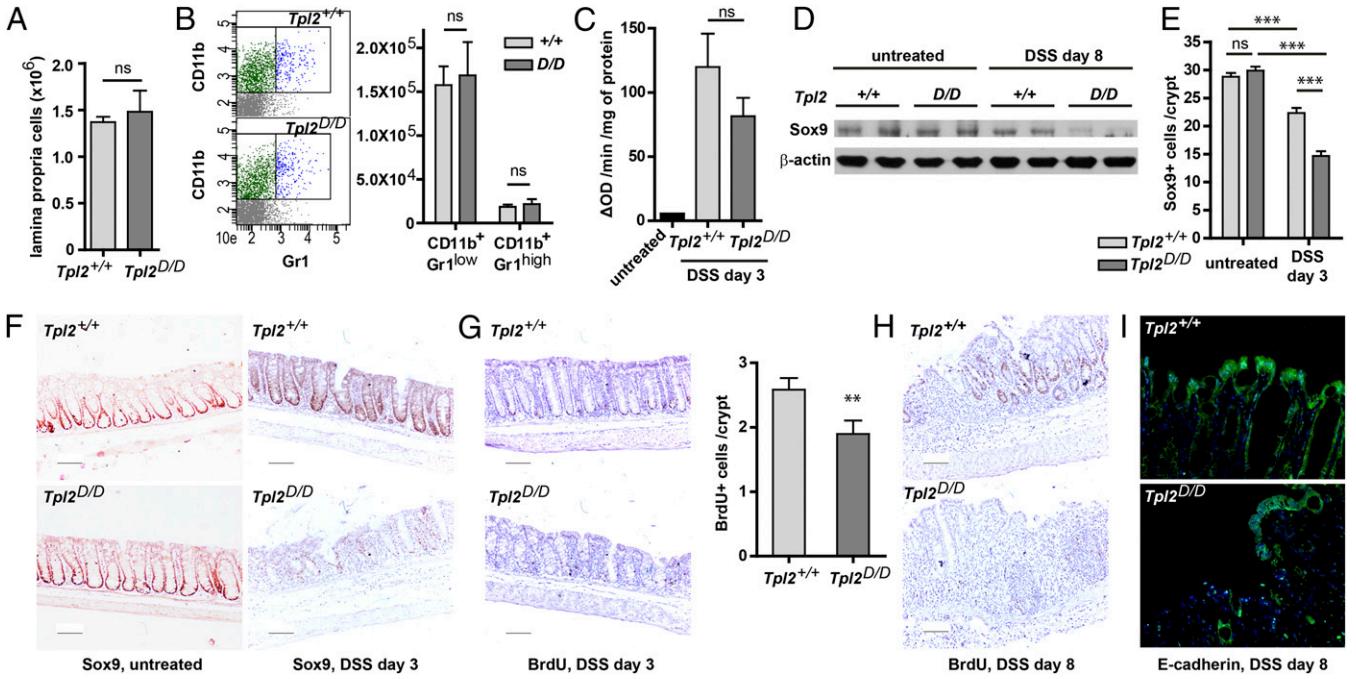

Fig. 2. Tpl2 is implicated in the mechanisms of epithelial homeostasis upon DSS treatment but is dispensable for inflammatory infiltration. (*A*) Quantification of isolated lamina propria cells in $Tpl2^{D/D}$ mice ($n = 4$) and WT controls ($n = 4$) on day 3.5 upon DSS treatment shows similar inflammatory infiltration. Indicative of two independent experiments. (*B*) Quantification of macrophages ($CD11b^+Gr1^{low}$) and granulocytes ($CD11b^+Gr1^{hi}$) in the lamina propria by flow cytometry analysis. (*C*) $Tpl2^{D/D}$ mice ($n = 5$) and WT controls ($n = 5$) show similar myeloperoxidase activity in the colon on day 3 of DSS treatment. (*D*) Sox9 protein levels are reduced in the colons of $Tpl2^{D/D}$ mice on day 8 of DSS treatment compared with DSS-treated WT controls and untreated mice. (*E*) Quantification of $Sox9^+$ cells in the crypts of untreated and DSS-treated $Tpl2^{D/D}$ and WT control mice by immunostaining as displayed in *F*. $Sox9^+$ cells in the crypts are reduced following DSS treatment, and Tpl2 deletion significantly enhances their loss. (*F*) Immunostaining for Sox9 in $Tpl2^{D/D}$ and WT control mice, untreated or DSS-treated for 3 d ($n = 3$–4 each), reveals crypts with markedly reduced $Sox9^+$ cells in $Tpl2^{D/D}$ mice. (Scale bars: 100 μm.) (*G*) Epithelial proliferation in $Tpl2^{D/D}$ mice ($n = 5$) and WT controls ($n = 6$) on day 3 of DSS treatment assessed by BrdU incorporation in the crypts. $Tpl2^{D/D}$ mice show significantly reduced numbers of BrdU-incorporating cells. (Scale bars: 100 μm.) (*H*) BrdU incorporation experiments on day 8 of DSS treatment show loss of alive crypts in $Tpl2^{D/D}$ mice ($n = 5$) in contrast to WT controls ($n = 5$) in which the crypts show proliferative activity. (*I*) $Tpl2^{D/D}$ mice ($n = 3$) show extensive epithelial cell depletion on day 8 shown by E-cadherin immunostaining. Nuclei are stained with DAPI. (Magnification: 200×.) All data shown represent mean ± SEM. Statistical significance was calculated with Student *t* test or Mann–Whitney test (***$P < 0.001$; **$P < 0.01$; ns, nonsignificant).

IEC death (*SI Appendix*, Fig. S6*C*). In addition, 9-mo-old $Tpl2^{D/D}$ mice have normal Paneth and Goblet cell populations in the ileum and the colon, indicating that there are no defects in mechanisms of epithelial differentiation (*SI Appendix*, Fig. S7). On the other hand, loss of crypts and ulceration may result from defects in mechanisms of compensatory epithelial proliferation. Notably, DSS-treated $Tpl2^{D/D}$ mice show reduced expression of Sox9 in the colon (Fig. 2*D*), which is a well-established crypt progenitor/stem cell marker (18). DSS treatment leads to an early reduction of $Sox9^+$ cells in the basal part of colonic crypts in WT mice. This reduction in $Sox9^+$ cells is significantly enhanced in $Tpl2^{D/D}$ mice leading to areas with severe depletion of $Sox9^+$ cells (Fig. 2 *E* and *F*). To examine whether this reduction of $Sox9^+$ cells reflects early proliferation defects, we monitored epithelial proliferation by BrdU-pulse administration experiments on experimental day 3. These experiments showed significantly reduced cells incorporating BrdU (cells in S-phase) in the crypts of $Tpl2^{D/D}$ mice compared with WT littermates (Fig. 2*G*). A defect in epithelial cell proliferation was even more prominent later on day 8 (Fig. 2*H*), resulting in a vast depletion of the epithelial monolayer in $Tpl2^{D/D}$ mice (Fig. 2*I*). These results suggest a physiologically relevant implication of Tpl2 in mechanisms of compensatory epithelial proliferation in response to injury. This function is similar to that of Myd88 and TLR4, which are upstream activators of Tpl2 and also promote compensatory proliferation in the intestinal epithelium protecting from experimental colitis (19, 20) through still unidentified cellular mechanisms. These results raised the question on the specific cellular and molecular pathways through which Tpl2 promotes compensatory proliferation.

Conditional Inactivation of Tpl2 Reveals a Critical Homeostatic Role of Intestinal Myofibroblasts in Epithelial Response to Injury. To examine the cellular pathways mediating the homeostatic role of Tpl2 in the colon we generated mice bearing myeloid lineage-specific Tpl2 ablation ($Tpl2^{MYEL\text{-}KO}$) using *LysMCre* (21) mice (*SI Appendix*, Fig. S8 *A*–*C*) and mice bearing IEC-specific Tpl2 ablation ($Tpl2^{IEC\text{-}KO}$) using *VillinCre* (22) mice (*SI Appendix*, Fig. S9 *A* and *B*). Both $Tpl2^{MYEL\text{-}KO}$ mice and $Tpl2^{IEC\text{-}KO}$ mice showed similar responses to DSS-induced epithelial injury compared with the respective $Tpl2^{FL/FL}$ littermate controls (thereafter referred as $Tpl2^{FL}$ mice) in terms of weight loss, disease activity index, colon length, and histological features of colitis (Fig. 3 *A*–*F* and *SI Appendix*, Figs S8 and S9), arguing against a homeostatic role of Tpl2 through macrophages, granulocytes, or IECs.

Intestinal subepithelial myofibroblasts (IMFs) are mesenchymal cells which underlie the epithelium in close proximity to the crypts, where they participate in stem cell niche formation and developmental processes (23–26). To examine whether the reduction of $Sox9^+$ cells and the defective epithelial proliferation in $Tpl2^{D/D}$ mice result from a mesenchymal cell-mediated mechanism, we used *ColVICre* transgenic mice, which express Cre recombinase in IMFs (27), to generate $ColVICreTpl2^{FL/FL}$ mice ($Tpl2^{IMF\text{-}KO}$) bearing inactivation of Tpl2 in IMFs as shown previously (28). Remarkably, DSS administration in $Tpl2^{IMF\text{-}KO}$ mice led to an exacerbated colitis phenotype characterized by significantly increased weight loss,

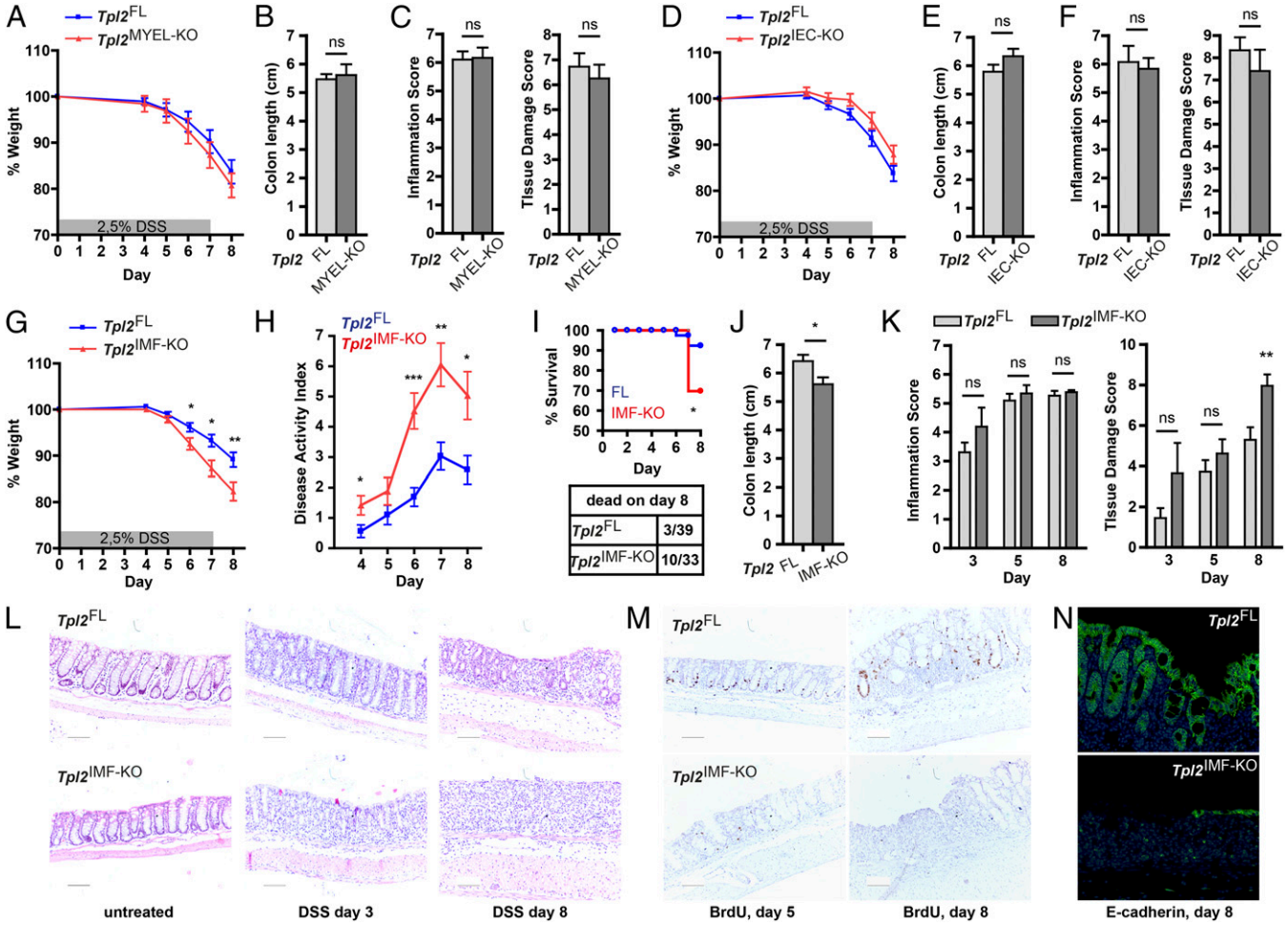

Fig. 3. Tpl2 ablation in intestinal myofibroblasts, but not in myeloid lineage or intestinal epithelial cells, is sufficient to confer increased susceptibility to DSS-induced colitis. (*A–C*) Myeloid-specific $Tpl2^{MYEL\text{-}KO}$ ($n = 14$) and $Tpl2^{FL}$ control mice ($n = 16$) treated with 2.5% DSS in two independent experiments show similar weight loss, colon length on day 8, and histopathological features. (*D–F*) Epithelial-specific $Tpl2^{IEC\text{-}KO}$ ($n = 17$) and $Tpl2^{FL}$ control mice ($n = 18$) treated with 2.5% DSS in three independent experiments show similar weight loss, colon length on day 8, and histopathological features. (*G–L*) $Tpl2^{IMF\text{-}KO}$ ($n = 33$) and $Tpl2^{FL}$ control mice ($n = 39$) were treated with 2.5% DSS in six independent experiments. $Tpl2^{IMF\text{-}KO}$ mice show increased weight loss (*G*), disease activity index (*H*), and lethality (*I*) ($P = 0.02891$; Gehan–Wilcoxon test). (*J*) Reduced colon length on day 8 in $Tpl2^{IMF\text{-}KO}$ mice (n = 21) compared with $Tpl2^{FL}$ controls ($n = 24$) in three independent experiments. (*K*) Inflammation and tissue damage scores in DSS-treated $Tpl2^{IMF\text{-}KO}$ mice compared with $Tpl2^{FL}$ controls early on day 3 ($n = 4$ and 5, respectively), on day 5 ($n = 6$ and 5), and late on day 8 ($n = 18$ and 23). (*L*) $Tpl2^{IMF\text{-}KO}$ mice show early loss of crypts progressing to complete loss of crypts and extensive ulceration. H&E-stained sections. (Scale bars: 100 μm.) (*M*) $Tpl2^{IMF\text{-}KO}$ mice show reduced proliferation in the crypts monitored by BrdU incorporation (scale bars: 100 μm), and (*N*) extensive epithelial cell depletion on day 8 by E-cadherin immunostaining. (Magnification: 200×.) All data represent mean ± SEM. Student *t* test or Mann–Whitney test (*$P < 0.05$; **$P < 0.01$; ***$P < 0.001$; ns, nonsignificant).

disease activity index, and lethality (Fig. 3 *G–I*) and reduced colon length (Fig. 3*J*) compared with $Tpl2^{FL}$ controls. Histopathological analysis showed that $Tpl2^{\text{IMF-KO}}$ mice display similar inflammation but significantly increased tissue damage score with early loss of crypts on experimental day 3 progressing to extensive ulceration on experimental day 8 (Fig. 3 *K* and *L*). These results establish a phenotype similar to that observed in $Tpl2^{D/D}$ mice, demonstrating that selective inactivation of Tpl2 in IMFs is sufficient to confer increased susceptibility to DSS-induced colitis. BrdU-pulse administration experiments showed a defective proliferative response to injury in the epithelium of $Tpl2^{\text{IMF-KO}}$ mice at both an early and a late time point during DSS treatment (Fig. 3*M*) associated with extensive epithelial cell depletion (Fig. 3*N*). These results show that IMFs protect the colonic epithelium following DSS-induced injury through the activation of the Tpl2 pathway, suggesting a previously unknown dominant role for this cell type in the maintenance of epithelial homeostasis. The homeostatic role of IMFs via Tpl2 upon intestinal damage was further validated in a second experimental colitis model; 2,4,6-trinitro benzene sulfonic acid (TNBS)-induced colitis. $Tpl2^{\text{IMF-KO}}$ mice subjected to TNBS-induced colitis show an exacerbated pathology characterized by increased weight loss, loss of crypts, and ulceration, even also transmural ulceration and necrosis, reflected as high tissue damage histological score (*SI Appendix*, Fig. S10).

To examine the distribution of intestinal myofibroblasts in the colon upon epithelial injury we treated WT mice with DSS and performed immunostainings against alpha smooth muscle actin (α-SMA), a microfilament protein expressed by myofibroblasts but also by pericytes, muscularis mucosae smooth muscle cells, and lymphatic lacteal-associated smooth muscle cells of the lamina propria (23). We observed that the network of $\alpha\text{-SMA}^+$ mesencymal cells of the lamina propria is reorganized in the colon of DSS-treated mice in association with tissue damage progression. An accelerated redistribution of $\alpha\text{-SMA}^+$ cells is observed in $Tpl2^{D/D}$ DSS-treated mice in the early lesions occurring upon DSS injury (*SI Appendix*, Fig. S11).

Molecular Profiling of Tpl2 Deficient Intestinal Myofibroblasts and Further Analyses Show Deregulation of Arachidonic Acid Metabolism and Prostaglandin Production Pathways. To examine the molecular pathways underlying the homeostatic function of Tpl2 in myofibroblasts we isolated IMFs from $Tpl2^{D/D}$ and WT control mice and analyzed the signaling pathways and downstream molecular targets that may be affected. Tpl2 in IMFs is not required for ERK activation upon stimulation with IL-18 or

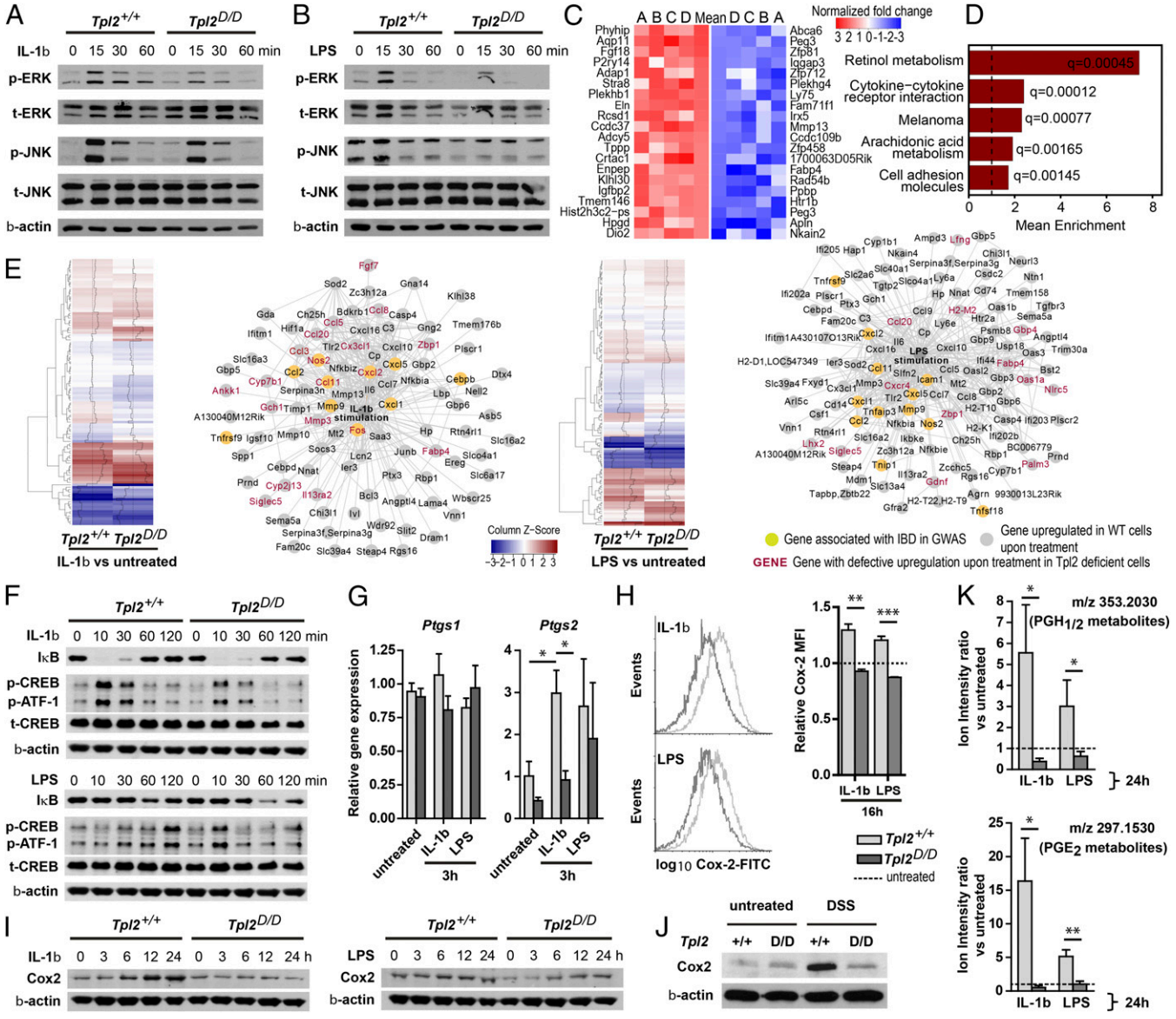

Fig. 4. Tpl2 in intestinal myofibroblasts mediates MAPK activation upon innate or inflammatory stimulation and is implicated in the activation of the Cox-2 pathway and arachidonic acid metabolism. (*A* and *B*) Western blots for phospho-ERK (p-ERK) and phospho-JNK (p-JNK) in IMFs isolated from $Tpl2^{D/D}$ and WT mice stimulated with IL-1β or LPS. (*C* and *D*) Gene expression profiling was performed by RNA-seq in primary nonstimulated IMFs isolated from $Tpl2^{D/D}$ and WT mice in four independent experiments (A to D). (*C*) Top and bottom 20 consistently deregulated genes are presented in a heat map. (*D*) Gene set enrichment analysis shows consistent enrichment of five KEGG pathways in genes deregulated in $Tpl2^{D/D}$ IMFs. (*E*) Tpl2 in IMFs partially mediates the induction of IL-1β or LPS-driven gene networks overlapping with the IBD-GWAS subnetwork downstream of IL-1β. Hierarchical clustering of genes consistently deregulated upon stimulation of IMFs with IL-1β or LPS in two independent experiments. Genes up-regulated in response to IL-1β or LPS are shown as STRING functional networks with highlighted genes showing defective up-regulation in $Tpl2^{D/D}$ IMFs and genes genetically associated with IBD in GWAS (2). (*F*) Western blots for IκB and phospho-CREB (p-CREB) in $Tpl2^{D/D}$ and WT IMFs stimulated with IL-1β or LPS. (*G*) RT-PCR for *Ptgs1* and *Ptgs2* gene expression levels in $Tpl2^{D/D}$ and WT IMFs stimulated with IL-1β or LPS ($n = 3$ each). (*H*) Cox-2 protein expression levels were measured by FACS analysis in IMFs stimulated with IL-1β or LPS for 16h ($n = 3$ each). Values represent relative mean fluorescence intensity (MFI) based on untreated controls. (*I*) Tpl2 is required for optimal Cox-2 up-regulation in IMFs upon stimulation with IL-1β or LPS as shown by Western blot. (*J*) Ex vivo validation of the Cox-2 pathway deregulation in the absence of Tpl2. $Tpl2^{D/D}$ and WT control mice (each $n = 2$ pooled) were treated for 6 d with 2.5% DSS or normal water, and stromal cells of the colon were isolated and cultured for 24 h without stimulation. Cox-2 protein levels were examined with Western blot. Indicative of two independent experiments. (*K*) Cox-2–mediated eicosanoids detected by mass spectrometry in supernatants of IL-1β or LPS-stimulated $Tpl2^{D/D}$ and WT IMFs ($n = 4$ each). Precursor ion mass (*m/z*) 297.1530 corresponds to PGE_2 metabolites (13,14-dihydro-tetranor-15-keto-PGE_2 and tetranor-PGE_1), and *m/z* 353.2030 corresponds to metabolites downstream of PGH_1 and PGH_2 (*SI Appendix, Methods*). Bars represent relative ion intensities compared with untreated controls. All data represent mean ± SEM. Student *t* test or Mann–Whitney test (*$P < 0.05$; **$P < 0.01$; ***$P < 0.001$; ns, nonsignificant).

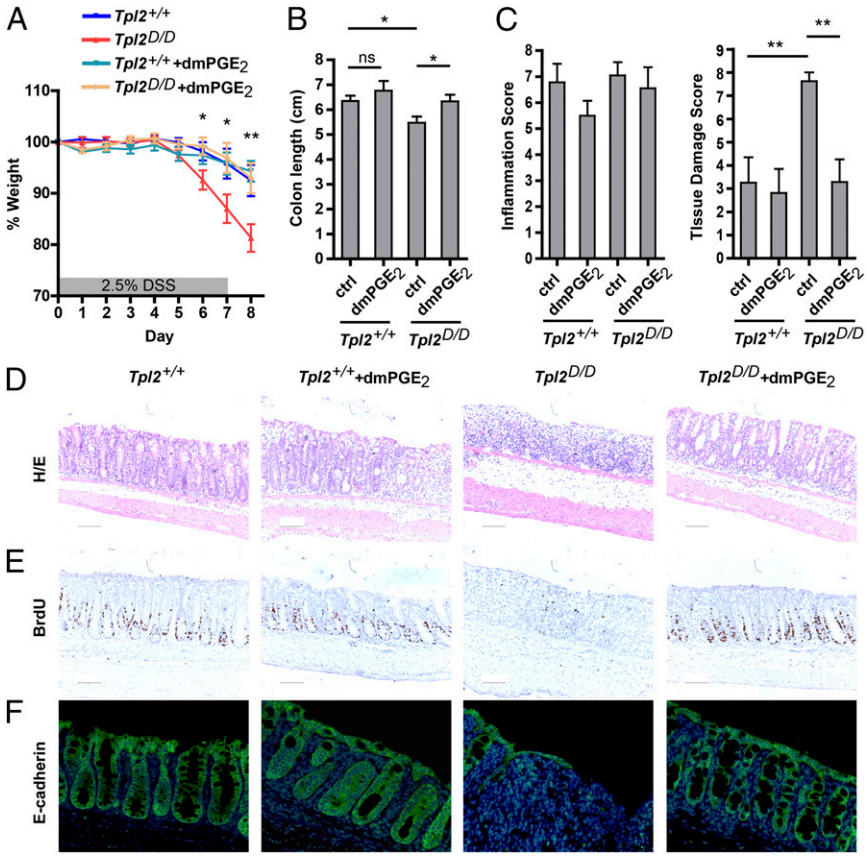

Fig. 5. Exogenous dmPGE$_2$ administration concurrently with DSS treatment rescues the exacerbated colitis phenotype of *Tpl2*$^{D/D}$ mice and restores epithelial proliferation and structure. Concurrently with 2.5% DSS treatment, *Tpl2*$^{D/D}$ ($n = 10$) and WT ($n = 11$) mice received i.p. injections of dmPGE$_2$ every 12 h at a dose of 10 μg/kg of body weight. Control (ctrl) *Tpl2*$^{D/D}$ ($n = 11$) and WT ($n = 10$) mice were similarly injected with saline. Data represent two independent experiments. (*A*) dmPGE$_2$ protects *Tpl2*$^{D/D}$ mice from increased weight loss observed in control *Tpl2*$^{D/D}$ mice (statistically compared), although it has no effect in WT mice. For days 6–8, Kruskal–Wallis *P* values are 0.0518, 0.0445, and 0.0083, respectively. (*B*) Colon length on experimental day 8. (*C*) Histopathological analysis on day 8. (*D*) dmPGE$_2$ rescues *Tpl2*$^{D/D}$ mice from the extensive loss of crypts and ulceration observed in control *Tpl2*$^{D/D}$ mice on day 8, although it has no effect in WT mice. H&E-stained sections. (Scale bars: 100 μm.) (*E*) dmPGE$_2$ protects *Tpl2*$^{D/D}$ mice from the defective epithelial proliferation observed in control *Tpl2*$^{D/D}$ mice on day 8, although it has no effect in WT mice as shown by BrdU incorporation experiments. (Scale bars: 100 μm.) (*F*) dmPGE$_2$ protects *Tpl2*$^{D/D}$ mice from the epithelial depletion observed in control *Tpl2*$^{D/D}$ mice on day 8, although it has no effect in WT mice as shown by E-cadherin immunostaining. Nuclei are stained with DAPI. (Magnification: 200×.) Data shown represent mean ± SEM. Student *t* test, Welch's *t* test, or Mann–Whitney test (*$P < 0.05$; **$P < 0.01$; ns, nonsignificant).

muramyl dipeptide, a NOD2 ligand (*SI Appendix*, Fig. S12), but it is required for ERK and to a less extent JNK activation upon stimulation with IL-1β (Fig. 4*A*) or LPS (Fig. 4*B*), similarly to its function described in other cell types (3). To gain insights into pathways mediated by Tpl2 in IMFs, we analyzed by RNA sequencing the expression profile of primary Tpl2$^{D/D}$ and WT IMFs, untreated or stimulated with IL-1β or LPS. Analysis of untreated Tpl2$^{D/D}$ IMFs in four independent experiments showed consistent deregulation of a subset of ∼40 genes at twofold expression levels (Fig. 4*C*). Gene set enrichment analysis performed in these expression data revealed a consistent deregulation of five KEGG pathways in the absence of Tpl2, namely, retinol metabolism, cytokine–cytokine receptor interaction, melanoma, arachidonic acid metabolism, and cell adhesion molecules (Fig. 4*D*). From genes which are down- or up-regulated in untreated Tpl2$^{D/D}$ IMFs we computationally inferred transcription factors which may mediate their activation such as CREB and the myogenesis-related Myog and Myod1, respectively (*SI Appendix*, Fig. S13). Furthermore, RNA sequencing in IMFs treated with IL-1β or LPS and functional network analysis of the genes induced showed that Tpl2 mediates in part the activation of both IL-1β and LPS-triggered networks (Fig. 4*E*). Several genes included in the IL-1β–induced Tpl2-mediated subnetwork, such as Nos2, Cxcl2, Ccl11, and the transcription factor Fos, are genetically associated with IBD in GWAS (Fig. 4*E*). Gene set enrichment analysis performed in Tpl2$^{D/D}$ IMFs treated with either IL-1β or LPS showed deregulation of several pathways related to fibroblast response to injury such as extracellular matrix, basement membrane, and wound healing (*SI Appendix*, Table S2). Computational analysis of genes up-regulated upon IL-1β or LPS treatment indicated AP1 and NFκB as the major transcription factors induced by these stimuli in both WT and Tpl2$^{D/D}$ IMFs (*SI Appendix*, Fig. S13). Relevant Western blot analysis showed that IκB is degraded early upon IL-1β and late upon LPS stimulation in both WT and Tpl2$^{D/D}$ IMFs (Fig. 4*F*). On the other hand, we verified by Western blot that Tpl2 mediates CREB activation in response to IL-1β and at a later time point in response to LPS in IMFs (Fig. 4*F*). The above results suggest implication of Tpl2 in multiple IMF functions and indicate potential pathways in which Tpl2 may be a dominant mediator with significant role at the level of intestinal physiology.

Among pathways deregulated in Tpl2 deficient IMFs, of particular interest for the mechanisms of epithelial homeostasis is arachidonic acid metabolism which involves production of prostaglandins by cyclooxygenases. Cox-2 in particular plays a homeostatic role in the epithelium, highlighted in *Cox-2*$^{-/-}$ mice which are highly susceptible to DSS-induced colitis exhibiting defective

epithelial proliferation due to impaired production of PGE_2, the major product of Cox-2 in colon epithelium (29, 30). Hydroxyprostaglandin dehydrogenase 15-(NAD) (Hpgd), a negative regulator of PGE_2 (31), is overexpressed in Tpl2 deficient IMFs (Fig. 4*C*). Tpl2 in IMFs mediates Cox-2 activation at the protein level in response to IL-1β and LPS as shown by Western blot and FACS analyses (Fig. 4 *H* and *I*). This effect involves defective transcriptional activation of the *Ptgs2* (*Cox-2*) gene downstream of IL-1β (Fig. 4*G*) in agreement with the role of Tpl2 in the activation of CREB (Fig. 4*F*), a transcription factor binding to *Ptgs2* promoter and mediating its transcription (32). Tpl2 deletion does not affect *Ptgs1* (*Cox-1*) gene expression levels in IMFs (Fig. 4*G*). To examine the in vivo relevance of these results we treated $Tpl2^{D/D}$ and WT control mice with 2.5% DSS or normal drinking water for 6 d and isolated stromal cells of the colon after epithelial cell depletion to measure the levels of spontaneous Cox-2 expression. In support of our in vitro results we observed impaired up-regulation of Cox-2 in cells isolated from DSS-treated $Tpl2^{D/D}$ mice (Fig. 4*J*). In agreement with the above-described role of Tpl2 in Cox-2 activation, $Tpl2^{D/D}$ IMFs stimulated with IL-1β or LPS show defective secretion of Cox-2–mediated eicosanoids, namely, PGE_2 metabolites and prostanoids downstream of PGH_1 and PGH_2, as analyzed by mass spectrometry (Fig. 4*K*). To specifically examine the role of Cox-2 in IMFs upon epithelial injury in vivo we generated $Cox\text{-}2^{IMF\text{-}KO}$ mice crossing *cox-2* conditional knockout mice (33) with *ColVICre* (27) mice. $Cox\text{-}2^{IMF\text{-}KO}$ mice treated with DSS showed significantly increased weight loss in the early phase of the protocol, on days 4 and 5, but not later on, indicating a homeostatic role of Cox-2 in IMFs early upon epithelial injury (*SI Appendix*, Fig. S14). Of note, Cox-2 in myeloid and endothelial cells also exerts a homeostatic role although in the late phase of the DSS colitis model (34). The above results collectively suggest a deregulation of the arachidonic acid metabolism–prostaglandin synthesis pathway in Tpl2 deficient IMFs which may underlie their defective homeostatic function upon epithelial injury in a mechanism partially mediated by Cox-2.

Exogenous PGE_2 Administration Rescues $Tpl2^{D/D}$ and $Tpl2^{IMF\text{-}KO}$ Mice from Increased Susceptibility to Colitis Restoring Epithelial Proliferation. The PGE_2 pathway is of particular physiological significance in humans highlighted by the fact that the *PTGER4* gene encoding the PGE_2 receptor EP4 shows strong genetic association with both forms of IBD (2). To assess in vivo the physiological significance of Cox-2-PGE_2 activation through Tpl2, we treated $Tpl2^{D/D}$ and WT mice concurrently with DSS and 16,16-dimethyl PGE_2 ($dmPGE_2$), a stable analog of endogenous PGE_2, or with saline as a control. $dmPGE_2$-treated WT mice showed similar weight loss to that of control WT mice in response to DSS (Fig. 5*A*), implying that exogenous $dmPGE_2$ at this dose does not protect from colitis when the endogenous PGE_2 production pathway is intact. By striking contrast, $dmPGE_2$ administration in $Tpl2^{D/D}$ mice led to rescue from the severe weight loss observed in control $Tpl2^{D/D}$ mice, leading to a clinical response similar to that observed in WT controls (Fig. 5*A*) and to a significantly rectified colon length (Fig. 5*B*). $dmPGE_2$ administration also rescued $Tpl2^{D/D}$ mice from the exacerbated tissue damage histological score (Fig. 5*C*), the extensive loss of crypts, and the widespread ulceration observed in $Tpl2^{D/D}$ controls, although it had no effect in WT controls (Fig. 5 *C* and *D*). No differences were observed in inflammation score with $dmPGE_2$ treatment (Fig. 5 *C* and *D*). Furthermore, measuring BrdU incorporation in crypts on experimental day 8 we observed that $dmPGE_2$ administration in $Tpl2^{D/D}$ mice led to restored epithelial proliferation and crypt survival similar to that of WT controls (Fig. 5*E*) protecting also the epithelium from excessive epithelial depletion (Fig. 5*F*). Therefore, PGE_2 acts as a major mediator downstream of Tpl2, able to rescue the functional defects observed in the epithelium in its absence. To examine this pathway in vivo specifically in IMFs we performed additional $dmPGE_2$ administration experiments in $Tpl2^{IMF\text{-}KO}$ mice. $dmPGE_2$ rescues the increased weight loss, tissue damage score, loss of crypts, and ulceration observed in DSS + saline-treated $Tpl2^{IMF\text{-}KO}$ mice (Fig. 6 *A*–*C*). $dmPGE_2$ also restores epithelial proliferation (Fig. 6*D*), protecting from epithelial depletion (Fig. 6*E*). These results establish the physiological significance of the activation of the Tpl2-Cox-2-PGE_2 pathway in IMFs upon epithelial injury. $dmPGE_2$ administration also rescues $TLR4^{-/-}$ mice (20) and $Myd88^{-/-}$ mice (30) from exacerbated colitis, but not WT controls, rescuing the specific defects observed in these mice in terms of epithelial proliferation. Thus, the Cox-2-PGE_2 pathway mediates the homeostatic function of innate microflora recognition in the gut. It remains unknown, however, which cellular pathways underlie this homeostatic role of innate recognition. Our present results suggest IMFs as a cellular link between innate recognition and homeostatic Cox-2-PGE_2 expression in the gut.

Intestinal Myofibroblasts Isolated from the Inflamed Ileum of IBD Patients Show Decreased *MAP3K8* Expression. In the inflamed mucosa of IBD patients, α-SMA–expressing mesenchymal cells show an altered and in some areas expanded distribution in the

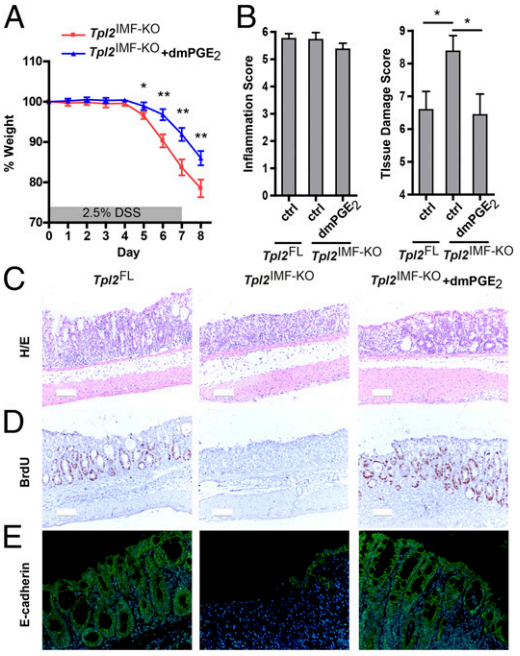

Fig. 6. Exogenous $dmPGE_2$ administration rescues the exacerbated DSS colitis phenotype of $Tpl2^{IMF\text{-}KO}$ mice and restores epithelial proliferation and structure. Concurrently with 2.5% DSS treatment, $Tpl2^{IMF\text{-}KO}$ (n = 24) received i.p. injections of $dmPGE_2$ every 12 h at a dose of 10 μg/kg of body weight. Control (ctrl) $Tpl2^{IMF\text{-}KO}$ mice (n = 21) were similarly injected with saline. Data represent three independent experiments. (*A*) Treatment with $dmPGE_2$ protects $Tpl2^{IMF\text{-}KO}$ mice from the weight loss observed in control $Tpl2^{IMF\text{-}KO}$ mice. (*B*) Histopathological analysis on day 8. Treatment with $dmPGE_2$ protects $Tpl2^{IMF\text{-}KO}$ mice from the extensive tissue damage observed in control $Tpl2^{IMF\text{-}KO}$ mice. No significant differences are observed in inflammation score. (*C*) Treatment with $dmPGE_2$ rescues $Tpl2^{IMF\text{-}KO}$ mice from the extensive loss of crypts and ulceration observed in control $Tpl2^{IMF\text{-}KO}$ mice on day 8. H&E-stained sections. (Scale bars: 100 μm.) (*D*) Treatment with $dmPGE_2$ protects $Tpl2^{IMF\text{-}KO}$ mice from the defective epithelial proliferation and the death of crypts observed in control $Tpl2^{IMF\text{-}KO}$ mice on day 8 as shown by BrdU incorporation experiments. (Scale bars: 100 μm.) (*E*) Treatment with $dmPGE_2$ protects $Tpl2^{IMF\text{-}KO}$ mice from the epithelial depletion observed in control $Tpl2^{IMF\text{-}KO}$ mice on day 8 as shown by E-cadherin immunostaining. Nuclei are stained with DAPI. (Magnification: 200×.) All data shown represent mean ± SEM. Student t test or Mann–Whitney test (*$P < 0.05$; **$P < 0.01$).

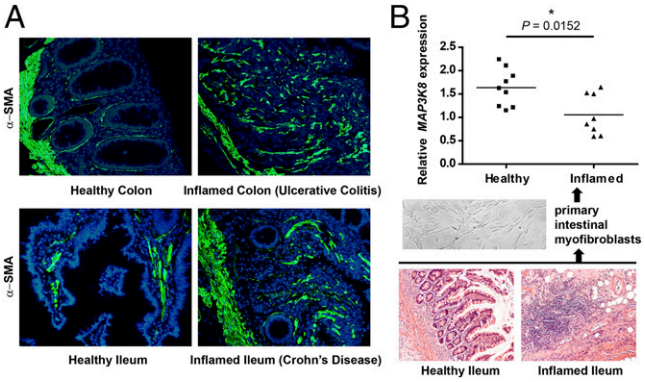

Fig. 7. *MAP3K8* is significantly down-regulated in IMFs isolated from the inflamed ileum of IBD patients. (*A*) The network of α-SMA$^+$ mesenchymal cells in the lamina propria is reorganized in the inflamed ileum and colon of IBD patients. Immunostainings for α-SMA were performed in paraffin sections of biopsies taken from patients suffering from Crohn's disease ($n = 6$) or ulcerative colitis ($n = 3$). Nuclei are stained with DAPI. (Magnification: 200×.) (*B*) IMFs were isolated from healthy and inflamed ileum tissues of IBD patients and control subjects ($n = 9$) (see *Materials and Methods* for clinical data). Indicative photomicrographs of primary IMF cultures and of H&E-stained sections of ileal biopsies from these patients are shown. (Magnification: 100×.) *MAP3K8* gene expression levels were measured by RT-PCR. Data shown represent mean ± SEM. Mann–Whitney test.

lamina propria (Fig. 7*A*), which is indicative of a potentially active involvement of these populations in disease processes. Subepithelial IMFs are a major α-SMA$^+$ mesenchymal cell type in the lamina propria showing high plasticity and a complex origin from several other mesenchymal but also nonmesenchymal cell types (23). The above analyses performed in mouse models strongly suggest a cell-specific homeostatic role of the Tpl2 pathway in IMFs. To determine the relevance of this mechanism to the complex human situation we performed a series of IMF isolations from healthy and inflamed tissues, ileum and colon, from patients diagnosed with either Crohn's disease ($n = 9$) or ulcerative colitis ($n = 9$) undergoing surgery. IMFs isolated from healthy tissues of colorectal cancer or diverticulosis patients ($n = 5$) were used as additional controls. *MAP3K8* gene expression was significantly reduced in IMFs isolated from the inflamed ileum of IBD patients compared with IMFs isolated from healthy ileal tissues (Fig. 7*B*). No significant difference in *MAP3K8* expression was observed in IMFs isolated from the inflamed colon of IBD patients (*SI Appendix*, Fig. S15*A*). Reduced *MAP3K8* gene expression in IMFs in the inflamed ileum appears to be cell-specific because *MAP3K8* expression is slightly increased in peripheral blood mononuclear cells from IBD patients compared with control subjects (*SI Appendix*, Fig. S15*B*). *PTGS2* but not *PTGS1* gene expression levels correlate with *MAP3K8* expression in cultured IMFs isolated from the ileum of Crohn's disease patients (*SI Appendix*, Fig. S16*A*). This correlation is also observed in snap frozen biopsies from IBD patients but not from healthy control subjects (*SI Appendix*, Fig. S16*B*). The mechanistic details of *MAP3K8–PTGS2* interaction in human IMFs need further investigation, however. The down-regulation of *MAP3K8* gene expression in IMFs in the inflamed intestine of IBD patients underlines the physiological relevance of this cellular and molecular pathway to human disease.

Collectively, our results establish a mechanism in which IMFs sense the innate signals and the inflammatory milieu formed in the pericryptal area upon epithelial damage, to activate the Tpl2-Cox-2-PGE_2 pathway which promotes compensatory epithelial proliferation in the crypts and intestinal homeostasis. Comparison of IBD GWAS results with this pathway shows involvement of five IBD-associated genes functionally connecting *MAP3K8* with *IL1R1*, *MAPK1*, *NFKB1*, and *PTGER4* genes (Fig. 8).

Discussion

Our results reveal an IMF-specific homeostatic mechanism which may be highly relevant to human IBD. The *MAP3K8* gene is located in a high linkage disequilibrium region bordered by two recombination hot spots (*SI Appendix*, Fig. S1*A*). The IBD-associated SNP rs1042058 shows between-study heterogeneity of odds ratios; thus, it is a genetic marker of this genetic block rather than a causative variant itself. ENCODE data provide clues for candidate causative variants in linkage disequilibrium with rs1042058 (*SI Appendix*, Fig. S1*B*). Cis-eQTL analysis performed in the high linkage disequilibrium region around *MAP3K8* revealed one deletion and 13 SNPs whose minor frequency alleles are associated with diminished *MAP3K8* expression in human cells. A subset of these SNPs is localized inside regulatory elements active in the normal human colonic mucosa (*SI Appendix*, Fig. S17). On the other hand, search in current human genomic variation data revealed at least 12 rare variants in the *MAP3K8* gene (minor allele frequency < 0.01), either missense, splice, or frameshift variants, which are predicted to exert a deleterious effect in Tpl2 protein (*SI Appendix*, Table S3). Further investigation is required, however, to identify the genetic variation(s) in the *MAP3K8* gene conferring increased risk for IBD pathogenesis, either as common variants of small effect, such as eQTLs, or rare variants of large effect. It is also possible that the effect of *MAP3K8* in IBD risk relies on the accumulation of small effect variants in multiple genes of the PGE_2 production and sensing pathway as a whole.

The reduced *MAP3K8* gene expression we show in IMFs isolated from the ileum of IBD patients may result from the physiological context of these cells in the inflamed intestine but possibly also from genetic factors such as the above-mentioned *MAP3K8* eQTLs and the fact that the CD-associated *NOD2* variant L1007fsinsC impairs *MAP3K8* activation in response to muramyl dipeptide in human cells (35). On the other hand, *MAP3K8* expression in the gut of ulcerative colitis patients from discordant twin pairs is negatively correlated with Firmicutes of the genus *Peptostreptococcus* (36), which are opportunistic pathogens and markers of dysbiosis in ulcerative colitis (37). In the unaffected

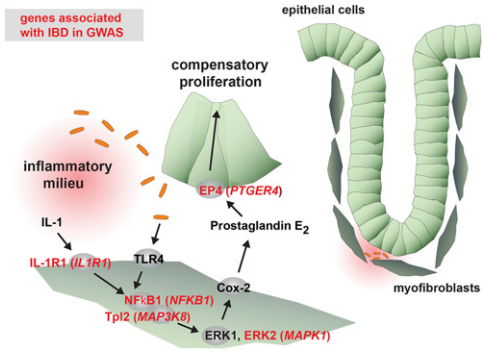

Fig. 8. Schematic representation of the mechanism proposed in the present study and the relevant genes which are genetically associated with IBD pathogenesis in humans. Following epithelial injury IMFs sense penetrating bacteria and the inflammatory milieu generated to activate a Tpl2-ERK-Cox-2-PGE_2–mediated homeostatic pathway and promote compensatory epithelial proliferation in the crypts. Indicated are genes genetically associated with IBD in recent GWAS (human symbols in parentheses) (2). These genes include *MAP3K8* encoding Tpl2 kinase, *NFKB1* encoding NF-κB1 (p105) which physically interacts with Tpl2 regulating its function and preventing its degradation (3), *MAPK1* encoding ERK2, *IL1R1* encoding IL-1 receptor, and the *PTGER4* gene encoding the PGE_2 receptor EP4.

siblings of the same study, *MAP3K8* expression was negatively correlated with *Faecalibacterium prausnitzii* (36), a commensal bacterium with anti-inflammatory function (38). Therefore, *MAP3K8* expression undergoes dynamic regulation in the human intestine in response to a combination of physiological, genetic, and microbial stimuli. The complex interconnection of such regulatory pathways may explain the fact that in our study, differential expression of *MAP3K8* expression was observed in IMFs isolated from the ileum but not from the colon of IBD patients.

Tpl2 is currently considered a well-established inflammatory mediator, with significant pharmacological interest for IBD (3). We have shown a relevant pathogenic implication of Tpl2 in $Tnf^{\Delta ARE}$ mice which spontaneously develop a chronic T-cell–mediated Crohn's-like IBD pathology in the ileum (7) without involvement of epithelial barrier disruption and restoration processes in which IMFs could play an important homeostatic role. Here we establish a homeostatic role for Tpl2 in IMFs in the context of epithelial injury-driven colitis. These contrasting roles suggested for Tpl2 by different animal models should be considered for effective therapeutic manipulation of the Tpl2 pathway in IBD. Of note, contrary to our results, a recent report indicated a pathogenic role for Tpl2 in DSS-induced colitis (39). This discrepancy could result from the different genetic background used or from experimental conditions such as the use of littermate and cohoused mice; the DSS model is particularly sensitive to these factors because the intestinal microflora is shaped through maternal transfer in a long-term manner (40) bearing transferrable colitogenic activity in the DSS model (41). To avoid microflora and genetic confounding, in the present study we performed our experiments using only large groups of littermate and cohoused mice as recommended (42, 43), which was not clarified in the study by Lawrenz et al. (39). In addition, Tpl2 inhibitor administration in DSS-treated C57BL/6 WT mice did not confer protection, compared with cohoused littermate controls, in contrast to the result reported by Lawrenz et al. for the same dosage (39) (*SI Appendix*, Fig. S18).

The dominant role of IMFs in the maintenance of epithelial homeostasis, directly linking innate sensing with epithelial proliferation and repair, is a surprising result of the present study. The exact cellular pathways underlying the homeostatic role of innate recognition in the gut remain to be identified, although increasing evidence suggests such a role for stromal cell types. A homeostatic function in the stroma has been shown for MyD88 (44) and NLRP3 (45). In addition, NLRP6, which also plays a homeostatic role in the gut, is highly expressed in IMFs (46). This key role of IMFs in epithelial homeostasis can be explained by their subepithelial localization and their physiological implication in mechanisms of epithelial proliferation and differentiation during development (23, 26). IMFs are in close proximity to the crypts participating in the construction of the stem cell niche (23, 24) where they secrete growth factors and morphogens required in developmental processes (25). PGE_2 interacts with Wnt signaling promoting stem cell survival and proliferation in tissue regeneration processes (47), and PGE_2 supplementation is required for optimal growth of isolated human colonic crypts in culture (48). The physiological significance of PGE_2 and its receptor PTGER4 in the intestinal epithelium is highlighted by the successful use of the PTGER4-agonist ONO-4819CD in a recent promising Phase-II clinical trial that showed histological improvement of ulcerative colitis patients refractory to 5-aminosalicylates (49). We hypothesize that innate stimulation-driven Tpl2-mediated Cox-2-PGE_2 expression in IMFs is part of an on/off switch mechanism conditionally activated to support crypt function under emergency conditions enhancing stem/progenitor cell survival and/or proliferation. Relevantly, a PGE_2-expressing population identified to be mesenchymal stem cells but not myofibroblasts (50) shows defective repositioning close to crypts in the rectum of DSS-treated $Myd88^{-/-}$ mice but not altered Cox-2 expression (30). However, the exact relationship between this population, intestinal fibroblasts, and myofibroblasts is not completely clear (51). The interplay between IMFs, other mesenchymal cells, and crypt function is an emerging field. Mesenchymal-specific genetic tools will be necessary to clarify these relationships, given the large variability and plasticity of mesenchymal populations in the lamina propria (23).

Another aspect of IMF biology is their implication in mechanisms promoting or protecting from tumorigenesis. We have relevantly shown that Tpl2 in IMFs regulates HGF production and protects from tumorigenesis induced by a protocol combining azoxymethane administration (a genotoxic-carcinogenic agent) with multiple cycles of DSS treatment (28). This HGF-mediated function of Tpl2 appears to be specific for the context of tumorigenesis because no differential expression of HGF is observed in the colon of $Tpl2^{D/D}$ and $Tpl2^{\text{IMF-KO}}$ mice upon acute DSS-induced epithelial injury at a time point when differences in epithelial proliferation are already observed (*SI Appendix*, Fig. S19*A*). $Tpl2^{D/D}$ and $Tpl2^{\text{IMF-KO}}$ mice show increased dysplasia but not tumorigenesis following chronic DSS treatment in a 50-d protocol without azoxymethane administration (*SI Appendix*, Fig. S19 *B–E*). Increased dysplasia may result from chronic proliferative responses compensating Sox-9^+ stem/progenitor cell loss occurring upon acute DSS treatment (Fig. 2 *E* and *F*), similar to the dysplastic effect of genetic Sox-9 ablation in epithelial cells (52). Therefore, Tpl2 is required early upon epithelial damage for intestinal homeostasis through the mechanisms shown in the present study, and its absence under conditions of chronic damage confers increased susceptibility to dysplasia and to mutagenesis-driven HGF-mediated tumor development.

The Tpl2-Cox-2-PGE_2 pathway is of high pharmacological interest for IBD with strategies aiming at either its inhibition as a means to dampen inflammatory responses [Cox-2, Tpl2 targeting (3)] or its activation as a means to promote mucosal healing (49, 51) (PGE_2 administration). Accumulation of mutations in the Tpl2-Cox-2-PGE_2 axis is predicted here to increase risk for IBD pathogenesis and to also prevent the effectiveness of therapies targeting these molecules as inflammatory mediators. The identification of the exact genetic variants underlying these associations will be essential for such patient stratification.

Materials and Methods

Generation and Characterization of *tpl2* Conditional Knockout Mice and *tpl2* Deficient Mice. The conditional *map3k8-tpl2* gene targeting strategy is shown in *SI Appendix*, Fig. S3*A*. The gene was isolated from a C57BL/6J mouse genome Bacterial Artificial Chromosome library (clone RP24-320F20). In a three-loxP vector containing a neomycin cassette (pEasyFlox) we inserted a 4.3-kb NotI-BamHI and a 3.1-kb XhoI-XhoI gene fragment as 5′- and 3′-homology arms, respectively. A 1.5-kb SalI-XbaI fragment containing the *tpl2* gene exon 4 was inserted between loxP sites 2 and 3. Excision of exon 4 deletes residues 169–254 of the Tpl2 protein and alters the reading frame for the rest of the transcript also truncating residues 255–467. Residues 169–467 encode the serine/threonine kinase active site and the kinase activation segment of Tpl2. The vector was electroporated into C57BL/6J mouse embryonic stem cells. Clones surviving from positive/negative selection were screened for 5′ and 3′ homologous recombination by Southern blot. One clone selected was microinjected into C57BL/6 albino blastocysts and transferred to pseudopregnant females in the transgenic facility of BSRC "Alexander Fleming." Chimeric mice bearing germ-line transmission ($Tpl2^{NFL/+}$) were bred to C57BL/6J mice. Crossing with EIIa-Cre transgenic mice (53) led to offspring with loxP1-loxP3 recombination (complete knockout allele, defloxed, $Tpl2^{D/+}$) and loxP1-loxP2 recombination (conditional knockout allele without the neomycin cassette, floxed, $Tpl2^{FL/+}$), which were validated with Southern blot and selected as colony founders (*SI Appendix*, Fig. S3*B*). Mice on a mixed C57BL/6J-129sv genetic background were generated upon breeding with 129sv mice. Genotyping primers were loxp3s 5′-GTTTTCACCTGACTGCTCCC-3′ and loxp3a 5′-AGCATTTCCAGACCATCACC-3′ (Flox allele 368 bp, WT 307 bp), and loxp1s 5′-ATGGCTTTGTGGGATTGTTGTTCC-3′ and loxp3a (Deflox allele 653 bp).

Tpl2$^{D/D}$ mice were born at the expected Mendelian ratio, developed normally, and were fertile. The efficient inactivation of *tpl2* gene was verified at the mRNA and protein level (*SI Appendix*, Fig. S3 *C* and *D*). Macrophages isolated from *Tpl2*$^{D/D}$ mice showed defective ERK activation upon LPS administration and impaired TNF secretion (*SI Appendix*, Fig. S3 *E* and *F*) as originally observed in *Tpl2*$^{-/-}$ mice (4). *Tpl2*$^{D/D}$ mice were also resistant to the TNF-dependent LPS/D-galactosamine lethal endotoxic shock similarly to *Tpl2*$^{-/-}$ mice (4) (*SI Appendix*, Fig. S3*G*). These results establish a new genetic tool for the study of cell-specific functions of Tpl2 in vivo.

Study Approval. All mice were used in accordance with the guidance of the Institutional Animal Care and Use Committee of BSRC "Alexander Fleming." Human studies were approved by the Ethical Committee of Istituto Clinico Humanitas. All participants were provided with complete information about the study.

ACKNOWLEDGMENTS. We thank S. Lalos and A. Katevaini for technical assistance in histopathology, P. Athanasakis and N. Giannakas for technical assistance, P. Chouvardas for computational assistance, V. Harokopos and M. Reczko for assistance in the RNA-seq experiment and detection of differentially expressed genes, M. Samiotaki for assistance in mass spectrometry, T. Fotsis and A. S. Politou (University of Ioannina) for advice, and A. Dimas and L. Jostins (Wellcome Trust Sanger Institute) for helpful discussions on IBD genetics. This work was supported by Hellenic Ministry of Education Grants PENED-03EΔ770 (to G.K.) and GSRT LS4-69 (to J.R.); Synergasia I Program "Systems Biology" (J.R.); and European Commission Seventh Framework Programs INFLA-CARE 223151 (G.K.), GENPRO Grant 245497 (to J.R.), Advanced European Research Council Project MCs-inTEST 340217 (G.K.), and the Innovative Medicines Initiative-funded Project "BeTheCure" 115142-2 (G.K. and S.D.). The authors also thank the InfrafrontierGR Infrastructure 2007-2013 (MIS 423575) for providing services and equipment.

1. Kaser A, Zeissig S, Blumberg RS (2010) Inflammatory bowel disease. *Annu Rev Immunol* 28:573–621.
2. Jostins L, et al.; International IBD Genetics Consortium (IIBDGC) (2012) Host-microbe interactions have shaped the genetic architecture of inflammatory bowel disease. *Nature* 491(7422):119–124.
3. Gantke T, Sriskantharajah S, Sadowski M, Ley SC (2012) IκB kinase regulation of the TPL-2/ERK MAPK pathway. *Immunol Rev* 246(1):168–182.
4. Dumitru CD, et al. (2000) TNF-alpha induction by LPS is regulated posttranscriptionally via a Tpl2/ERK-dependent pathway. *Cell* 103(7):1071–1083.
5. Mielke LA, et al. (2009) Tumor progression locus 2 (Map3k8) is critical for host defense against Listeria monocytogenes and IL-1 beta production. *J Immunol* 183(12): 7984–7993.
6. Watford WT, et al. (2008) Tpl2 kinase regulates T cell interferon-gamma production and host resistance to Toxoplasma gondii. *J Exp Med* 205(12):2803–2812.
7. Kontoyiannis D, et al. (2002) Genetic dissection of the cellular pathways and signaling mechanisms in modeled tumor necrosis factor-induced Crohn's-like inflammatory bowel disease. *J Exp Med* 196(12):1563–1574.
8. Cohen P (2009) Targeting protein kinases for the development of anti-inflammatory drugs. *Curr Opin Cell Biol* 21(2):317–324.
9. Eliopoulos AG, Wang CC, Dumitru CD, Tsichlis PN (2003) Tpl2 transduces CD40 and TNF signals that activate ERK and regulates IgE induction by CD40. *EMBO J* 22(15): 3855–3864.
10. Lin X, Cunningham ET, Jr, Mu Y, Geleziunas R, Greene WC (1999) The proto-oncogene Cot kinase participates in CD3/CD28 induction of NF-kappaB acting through the NF-kappaB-inducing kinase and IkappaB kinases. *Immunity* 10(2):271–280.
11. Das S, et al. (2005) Tpl2/cot signals activate ERK, JNK, and NF-kappaB in a cell-type and stimulus-specific manner. *J Biol Chem* 280(25):23748–23757.
12. Fukata M, et al. (2005) Toll-like receptor-4 is required for intestinal response to epithelial injury and limiting bacterial translocation in a murine model of acute colitis. *Am J Physiol Gastrointest Liver Physiol* 288(5):G1055–G1065.
13. Roulis M, Armaka M, Manoloukos M, Apostolaki M, Kollias G (2011) Intestinal epithelial cells as producers but not targets of chronic TNF suffice to cause murine Crohn-like pathology. *Proc Natl Acad Sci USA* 108(13):5396–5401.
14. Axelsson LG, Landström E, Goldschmidt TJ, Grönberg A, Bylund-Fellenius AC (1996) Dextran sulfate sodium (DSS) induced experimental colitis in immunodeficient mice: Effects in CD4(+) -cell depleted, athymic and NK-cell depleted SCID mice. *Inflamm Res* 45(4):181–191.
15. Serebrennikova OB, et al. (2012) Tpl2 ablation promotes intestinal inflammation and tumorigenesis in Apcmin mice by inhibiting IL-10 secretion and regulatory T-cell generation. *Proc Natl Acad Sci USA* 109(18):E1082–E1091.
16. Xiao Y, et al. (2014) TPL2 mediates autoimmune inflammation through activation of the TAK1 axis of IL-17 signaling. *J Exp Med* 211(8):1689–1702.
17. Nenci A, et al. (2007) Epithelial NEMO links innate immunity to chronic intestinal inflammation. *Nature* 446(7135):557–561.
18. Furuyama K, et al. (2011) Continuous cell supply from a Sox9-expressing progenitor zone in adult liver, exocrine pancreas and intestine. *Nat Genet* 43(1):34–41.
19. Rakoff-Nahoum S, Paglino J, Eslami-Varzaneh F, Edberg S, Medzhitov R (2004) Recognition of commensal microflora by toll-like receptors is required for intestinal homeostasis. *Cell* 118(2):229–241.
20. Fukata M, et al. (2006) Cox-2 is regulated by Toll-like receptor-4 (TLR4) signaling: Role in proliferation and apoptosis in the intestine. *Gastroenterology* 131(3):862–877.
21. Clausen BE, Burkhardt C, Reith W, Renkawitz R, Förster I (1999) Conditional gene targeting in macrophages and granulocytes using LysMcre mice. *Transgenic Res* 8(4): 265–277.
22. Madison BB, et al. (2002) Cis elements of the villin gene control expression in restricted domains of the vertical (crypt) and horizontal (duodenum, cecum) axes of the intestine. *J Biol Chem* 277(36):33275–33283.
23. Powell DW, Pinchuk IV, Saada JI, Chen X, Mifflin RC (2011) Mesenchymal cells of the intestinal lamina propria. *Annu Rev Physiol* 73:213–237.
24. Ootani A, et al. (2009) Sustained in vitro intestinal epithelial culture within a Wnt-dependent stem cell niche. *Nat Med* 15(6):701–706.
25. Shaker A, Rubin DC (2010) Intestinal stem cells and epithelial-mesenchymal interactions in the crypt and stem cell niche. *Transl Res* 156(3):180–187.
26. Powell DW, Adegboyega PA, Di Mari JF, Mifflin RC (2005) Epithelial cells and their neighbors I. Role of intestinal myofibroblasts in development, repair, and cancer. *Am J Physiol Gastrointest Liver Physiol* 289(1):G2–G7.
27. Armaka M, et al. (2008) Mesenchymal cell targeting by TNF as a common pathogenic principle in chronic inflammatory joint and intestinal diseases. *J Exp Med* 205(2): 331–337.
28. Koliaraki V, Roulis M, Kollias G (2012) Tpl2 regulates intestinal myofibroblast HGF release to suppress colitis-associated tumorigenesis. *J Clin Invest* 122(11):4231–4242.
29. Morteau O, et al. (2000) Impaired mucosal defense to acute colonic injury in mice lacking cyclooxygenase-1 or cyclooxygenase-2. *J Clin Invest* 105(4):469–478.
30. Brown SL, et al. (2007) Myd88-dependent positioning of Ptgs2-expressing stromal cells maintains colonic epithelial proliferation during injury. *J Clin Invest* 117(1): 258–269.
31. Tai HH, Cho H, Tong M, Ding Y (2006) NAD+-linked 15-hydroxyprostaglandin dehydrogenase: Structure and biological functions. *Curr Pharm Des* 12(8):955–962.
32. Eliopoulos AG, Dumitru CD, Wang CC, Cho J, Tsichlis PN (2002) Induction of COX-2 by LPS in macrophages is regulated by Tpl2-dependent CREB activation signals. *EMBO J* 21(18):4831–4840.
33. Ishikawa TO, Herschman HR (2006) Conditional knockout mouse for tissue-specific disruption of the cyclooxygenase-2 (Cox-2) gene. *Genesis* 44(3):143–149.
34. Ishikawa TO, Oshima M, Herschman HR (2011) Cox-2 deletion in myeloid and endothelial cells, but not in epithelial cells, exacerbates murine colitis. *Carcinogenesis* 32(3):417–426.
35. Billmann-Born S, et al. (2011) Genome-wide expression profiling identifies an impairment of negative feedback signals in the Crohn's disease-associated NOD2 variant L1007fsinsC. *J Immunol* 186(7):4027–4038.
36. Lepage P, et al. (2011) Twin study indicates loss of interaction between microbiota and mucosa of patients with ulcerative colitis. *Gastroenterology* 141(1):227–236.
37. Rajilić-Stojanović M, Shanahan F, Guarner F, de Vos WM (2013) Phylogenetic analysis of dysbiosis in ulcerative colitis during remission. *Inflamm Bowel Dis* 19(3):481–488.
38. Sokol H, et al. (2008) Faecalibacterium prausnitzii is an anti-inflammatory commensal bacterium identified by gut microbiota analysis of Crohn disease patients. *Proc Natl Acad Sci USA* 105(43):16731–16736.
39. Lawrenz M, et al. (2012) Genetic and pharmacological targeting of TPL-2 kinase ameliorates experimental colitis: A potential target for the treatment of Crohn's disease? *Mucosal Immunol* 5(2):129–139.
40. Ubeda C, et al. (2012) Familial transmission rather than defective innate immunity shapes the distinct intestinal microbiota of TLR-deficient mice. *J Exp Med* 209(8): 1445–1456.
41. Elinav E, et al. (2011) NLRP6 inflammasome regulates colonic microbial ecology and risk for colitis. *Cell* 145(5):745–757.
42. Holmdahl R, Malissen B (2012) The need for littermate controls. *Eur J Immunol* 42(1): 45–47.
43. Chassaing B, Aitken JD, Malleshappa M, Vijay-Kumar M (2014) Dextran sulfate sodium (DSS)-induced colitis in mice. *Curr Protoc Immunol* 104:Unit 15.25.
44. Brandl K, et al. (2010) MyD88 signaling in nonhematopoietic cells protects mice against induced colitis by regulating specific EGF receptor ligands. *Proc Natl Acad Sci USA* 107(46):19967–19972.
45. Zaki MH, et al. (2010) The NLRP3 inflammasome protects against loss of epithelial integrity and mortality during experimental colitis. *Immunity* 32(3):379–391.
46. Normand S, et al. (2011) Nod-like receptor pyrin domain-containing protein 6 (NLRP6) controls epithelial self-renewal and colorectal carcinogenesis upon injury. *Proc Natl Acad Sci USA* 108(23):9601–9606.
47. Goessling W, et al. (2009) Genetic interaction of PGE2 and Wnt signaling regulates developmental specification of stem cells and regeneration. *Cell* 136(6):1136–1147.
48. Jung P, et al. (2011) Isolation and in vitro expansion of human colonic stem cells. *Nat Med* 17(10):1225–1227.
49. Nakase H, et al. (2010) Effect of EP4 agonist (ONO-4819CD) for patients with mild to moderate ulcerative colitis refractory to 5-aminosalicylates: A randomized phase II, placebo-controlled trial. *Inflamm Bowel Dis* 16(5):731–733.
50. Manieri NA, Drylewicz MR, Miyoshi H, Stappenbeck TS (2012) Igf2bp1 is required for full induction of Ptgs2 mRNA in colonic mesenchymal stem cells in mice. *Gastroenterology* 143(1):110–121 e110.
51. Powell DW, Saada JI (2012) Mesenchymal stem cells and prostaglandins may be critical for intestinal wound repair. *Gastroenterology* 143(1):19–22.
52. Bastide P, et al. (2007) Sox9 regulates cell proliferation and is required for Paneth cell differentiation in the intestinal epithelium. *J Cell Biol* 178(4):635–648.
53. Lakso M, et al. (1996) Efficient in vivo manipulation of mouse genomic sequences at the zygote stage. *Proc Natl Acad Sci USA* 93(12):5860–5865.